
Physical Implications of *RHESSI* Neutron Capture-Line Measurements

R. J. Murphy,¹ G. H. Share,¹ X.-M. Hua,² R. P. Lin,³ D. M. Smith,³ and R. A. Schwartz⁴

(1) *E.O. Hulburt Center for Space Research, Code 7650, Naval Research Lab., Washington, DC 20375, U.S.A.*

(2) *L3 Communications, EER Systems, Inc., Largo, MD 20774, U.S.A.*

(3) *Space Sciences Laboratory and Dep't. of Physics, University of California, Berkeley, CA 94720, U.S.A.*

(4) *NASA Goddard Space Flight Center, Greenbelt, MD 20771, U.S.A.*

Abstract

We report high spectral-resolution measurements of the 2.223 MeV neutron capture-line obtained with the *Reuven Ramaty High Energy Spectroscopic Imager (RHESSI)* from the 2002 July 23 solar flare. The measured time history is compared with predicted time histories calculated using a magnetic loop model with a magnetic field perpendicular to the solar surface at the footpoints. The derived constraints on the interacting-particle angular distribution imply that the particles suffered pitch-angle scattering during transport through the coronal portion of the loop. The photospheric $^3\text{He}/\text{H}$ ratio was not well-constrained, primarily due to uncertainties of the measured nuclear deexcitation-line flux used to represent the neutron-production time history.

1. Introduction

RHESSI detected the 2.223 MeV neutron capture-line from the 2002 July 23 solar flare. The line is formed when flare-produced neutrons are captured on photospheric hydrogen producing deuterium. Since the neutrons slow down before capture, the line is delayed by ~ 100 s. The delay is affected by both the photospheric ^3He abundance and the angular distribution of the interacting particles producing the neutrons. Neutron capture on ^3He produces no radiation but shortens the delay of the capture line [1]. Downward-directed interacting accelerated particles tend to produce neutrons deeper in the atmosphere where the higher density also shortens the delay.

In this paper we will use *RHESSI* observations of the neutron-capture line to determine the photospheric ^3He abundance by simultaneously varying both $^3\text{He}/\text{H}$ and the interacting-particle angular distribution. Previous analyses of neutron-capture line data assumed various analytic shapes for the interacting-

particle angular distribution. Here, neutron capture-line time histories are calculated using a physically-based magnetic loop model [2, 3] with a magnetic field perpendicular to the solar surface at the footpoints. The model includes magnetic mirroring in the convergent flux tube and MHD pitch-angle scattering (PAS) in the corona. The level of PAS is characterized by the isotropization mean-free-path Λ (expressed by λ , the ratio of Λ to the loop half-length). With no PAS ($\lambda \rightarrow \infty$), most particles are moving parallel to the solar surface when they interact (i.e., a “fan beam”). Scattering causes the loss cone to be continuously repopulated resulting in more downward-directed interacting particles. (See Figure 10 of [4].) PAS is assumed to be energy-independent.

We use new and updated neutron production kinematics and cross sections [3] and the loop model to calculate the neutron capture-line time history for various assumptions of the accelerated-particle power-law spectral index (s), the photospheric ${}^3\text{He}/\text{H}$ ratio, and the level of PAS (λ). We derive predicted neutron capture-line time histories by convolving the time histories calculated for instantaneous release with a neutron-production time history assumed to be given by the nuclear-deexcitation line flux measured for this flare (see below). The results summarized here are more fully discussed in [5].

2. Comparison of the *RHESSI* Data with the Calculations

The background-subtracted count spectrum measured by *RHESSI* near the neutron capture-line is shown in Panel (a) of Figure 1. The data were fit [6] with a model consisting of a Gaussian profile for the line, a broken power law for the electron bremsstrahlung and a nuclear deexcitation-line component, also shown in the Figure. *RHESSI* count spectra accumulated every 20 seconds were also fit with this model and the resulting capture-line and 4–7.6 MeV deexcitation-line time histories are shown in Panel (b) of Figure 1.

Because the 4.44 MeV ${}^{12}\text{C}$ line is weak and the 4–7.6 MeV deexcitation-line band is sensitive to the assumed abundances, we do not determine the spectral index from the data. Instead we assume two reasonable [7] spectral indexes (3.5 and 4.5) and vary ${}^3\text{He}/\text{H}$ from 0.1 to 20×10^{-5} and PAS from none ($\lambda \rightarrow \infty$) to strong ($\lambda = 20$). We also considered an angular distribution that is 100% downward-beamed. For each combination of index, ${}^3\text{He}/\text{H}$, and angular distribution, a predicted neutron capture-line time history was calculated and compared with the data, normalized to minimize χ^2 . Confidence levels for ${}^3\text{He}/\text{H}$ and λ were established assuming two parameters of interest [8].

The minimum χ^2 achieved (χ_{min}^2) was the same for both spectral indexes (60.0 for 44 degrees of freedom, or a confidence level of 5%). Panel (b) of Figure 1 shows the measured and best-fit predicted time histories for $s = 4.5$. For each s , Figure 2 shows how $\Delta\chi^2$ (the change of χ^2 from χ_{min}^2) varies as λ and ${}^3\text{He}/\text{H}$ are varied. For these two indexes, the results for λ (panel a) do not depend

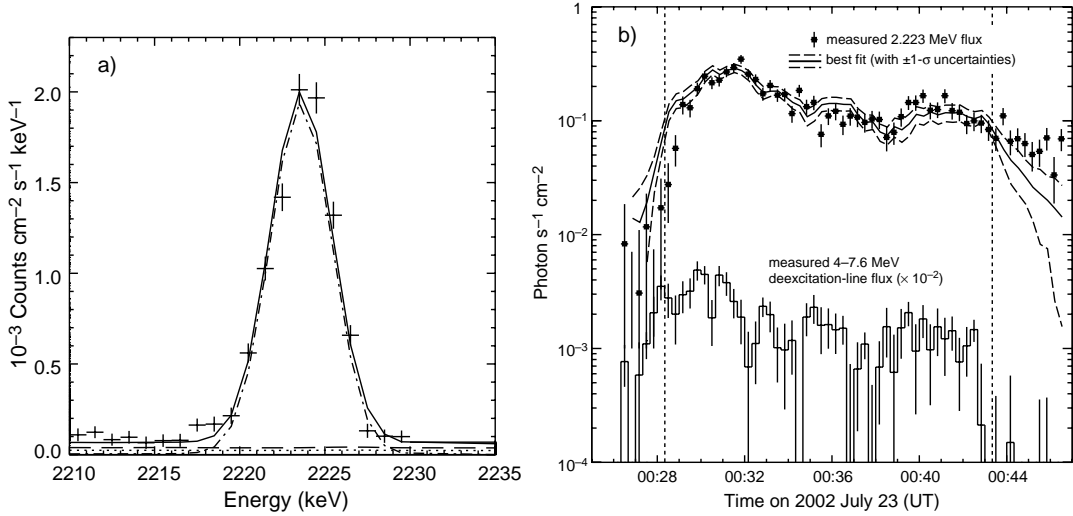


Fig. 1. *Panel a.* The observed 2.223 MeV neutron-capture line count spectrum accumulated over the bulk of the flare and the best fit to the data. The dotted curve is the nuclear component, the dashed curve is the bremsstrahlung power law, and the dashed-dotted curve is the line Gaussian. The solid curve is the sum of all of the components. *Panel b.* Measured time dependences of the 2.223 MeV neutron capture-line and the 4–7.6 MeV deexcitation-line fluxes. Also shown is the comparison of the best-fitting predicted neutron capture-line flux for $s = 4.5$ and the measured time history. The dotted lines indicate the time interval over which χ^2 was calculated (00:28:20–00:43:20 UT).

strongly on index. (In contrast to other consequences of the angular distribution such as deexcitation-line shifts [9].) χ^2_{\min} is achieved at $\lambda = 2000$ with a $1-\sigma$ allowable range of 700–5000 and a 99%-confidence upper-limit of ~ 7000 . PAS levels from weak to none can therefore be rejected. On the other hand, while more strongly downward-directed distributions ($\lambda < 700$) result in worse fits, even strong PAS cannot be rejected. However, the minimum χ^2 achieved assuming a 100% downward-beamed angular distribution was 68.3, or $\Delta\chi^2 = 8.3$ which can be rejected with better than 98% confidence. [9] found that a 100% downward-beam was required to produce the strong deexcitation-line red shifts observed for this flare unless the magnetic loop is inclined toward the Earth. Calculations of neutron capture-line production for inclined magnetic fields have not yet been performed, but longer decay times can reasonably be expected from inclined fields.

Figure 2 shows that a higher value of ${}^3\text{He}/\text{H}$ is required for the steeper spectrum (larger s). The total allowable range of ${}^3\text{He}/\text{H}$ ($1-\sigma$, two parameters of interest) over the range of indexes assumed here was from 0.5 to 10×10^{-5} . (${}^3\text{He}/\text{H}$ obtained from previous analyses of other flare data ranged from 0 to 5×10^{-5} .) If the spectral index could be determined by an independent method

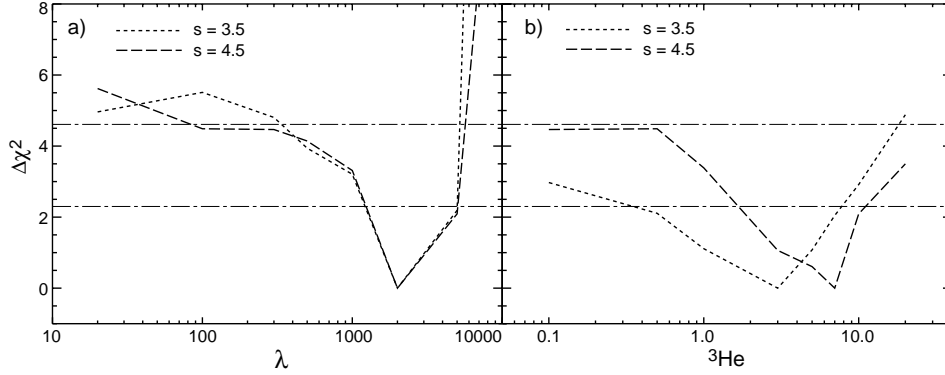


Fig. 2. Dependence of $\Delta\chi^2 = \chi^2 - \chi_{\min}^2$ for λ (panel a) and ${}^3\text{He}/\text{H}$ (panel b) for $s = 3.5$ (dotted) and 4.5 (dashed). The dotted-dashed lines indicate $\Delta\chi^2 = 2.3$ and 4.61 (68% and 90% confidence level for 2 parameters).

(e.g., γ -ray line fluence ratios), this allowable range would be reduced. However, we find that most of the uncertainty expressed in Figure 2 arises from the large statistical errors of the nuclear-deexcitation line flux used to represent the neutron-production time history (see Panel b of Figure 1).

This work was supported by NASA DPR S13,777G. The work at the UCB and NASA Goddard was supported by NASA contract NAS 5-98033.

3. References

1. Wang H.T., & Ramaty R. 1974, *Sol. Phys.*, 36, 129
2. Hua X.-M., Ramaty R., & Lingenfelter R.E. 1989, *ApJ*, 341, 516
3. Hua X.-M., Kozlovsky B., Lingenfelter R.E., Ramaty R. & Stupp A. 2002, *ApJS*, 140, 563
4. Share G.H., Murphy R.J., Kiener K. & de Sereville N. 2002, *ApJ*, 573, 464
5. Murphy R.J., Share G.H., Hua X.-M., Lin R.P., Smith D.M., & Schwartz R.A. 2003, accepted to *ApJL*
6. Share G.H., Murphy R.J., Smith D.M., Lin R.P., Shih A.Y., Hudson H., Schwartz R.A., & Kozlovsky B. 2003, accepted to *ApJL*
7. Ramaty R., Mandzhavidze N., & Kozlovsky B. 1996, in *High Energy Solar Physics*, ed. R. Ramaty, N. Mandzhavidze, & X.-M. Hua (New York:Am. Inst. Phys.), 374, 172
8. Lampton M., Margon B., & Bowyer S. 1976, *ApJ*, 208, 177
9. Smith D.M., Share G.H., Murphy R.J., Schwartz R.A., Shih A.Y., & Lin R.P. 2003, submitted to *ApJL*